Theoretical Study of Structural and Electronic Properties of Naked Stoichiometric and Nonstoichiometric Indium Phosphide Clusters

Sudip Roy[†] and Michael Springborg*

Physikalische Chemie, Universität des Saarlandes, D-66123 Saarbrücken, Germany

Received: October 4, 2002; In Final Form: January 14, 2003

In this paper results of calculations of structural and electronic properties of stoichiometric and nonstoichiometric indiumphosphide clusters with up to around 200 atoms are reported. The calculations were carried through using a simplified LCAO-DFT-LDA-TB scheme. We studied finite spherical parts of the zinc blende and wurtzite crystals, which were allowed to relax to the closest local-energy-minimum structure. For both the relaxed and unrelaxed structure, structural and electronic properties were analyzed. This procedure enables us to identify general and size-dependent properties. The properties of our interest include Mulliken populations, density of states, the HOMO−LUMO gap, the relative total energy, the spatial distribution of the frontier orbitals, and the structural relaxations.

Introduction

For the last two decades very much attention has been devoted to nanostructures of technologically relevant II−VI and III−V semiconductors spanning the range from properties of single nanocrystal structures to collective effects of their assemblies as well as size-dependent optical and electronic properties of semiconductor nanocrystals and nanorods. One of the most important issues, from the point of view both of fundamental understanding and as a means for varying the properties in a controlled way, is the evolution of the properties with size and stoichiometry from the molecular regime to the solid state, for instance, for III−V semiconductor nanocrystals.[1,2]

Indium phosphide (InP), as a representative III−V semiconductor, has been studied extensively and is of considerable interest for the semiconductor industry. This interest has its roots in its electronic properties and its excellent lattice match with low-band-gap alloys such as GaInAs and GaInAsP.[3] Thus, InP-based high-speed login circuits that take advantages of the high electron mobility in InP have been reported.[4] Furthermore, millimeter-wave sources and amplifiers based on InP are expected to operate at high frequencies with lower noise and higher frequency than those based on GaAs because of the larger separation between Γ and the *L* conduction band minimum.[5] Moreover, p-type InP has also found use in the fabrication of high-frequency Schottky-barrier solar cells.[6] Finally, InP-based devices are also very promising for application in optical fiber communications.[7]

Like other II−VI and III−V semiconductors InP may crystalize in either the zinc blende or the wurtzite crystal structure (for a general discussion of this near-degeneracy, see, e.g., ref 8). For crystalline InP the zinc blende structure is more stable than the wurtzite; i.e., experimentally produced samples show a higher percentage of the zinc blende than of the wurtzite structure.[9] However, only little is known about the structure of finite InP clusters and, in particular, the above-mentioned near-degeneracy of the zinc blende and wurtzite structures suggests that the structure of the finite clusters may depend critically on the size of the cluster.

Moreover, the fact that a large fraction of the total number of atoms are in the closest vicinity of the surfaces for the clusters makes the electronic properties depend critically on the structure of the surfaces which, in turn, may be quite different from that of the inner parts of the clusters. Generally, although semiconductor clusters in the size range 10−100 nm show bulk crystalline structures, they display markedly size-dependent electronic and optical properties. These are controlled by a combination of quantum confinement[11−15] and surface effects, and they offer a great opportunity to design new materials with tailor-made optical properties.

However, the fairly large size of the clusters (from some 10s to several 1000s of atoms) makes detailed theoretical studies of structural and electronic properties demanding and one has to restore to various approximations. Most often, it is assumed that the structure of the clusters is identical to that of a finite part of the infinite crystal, e.g., as finite spherical, cubic, or other polyhedral parts of the zinc blende structures for InP (see, e.g., refs 16−18 and references therein) and essentially no attempt has been made to use total-energy calculations in determining their structure. It is the purpose of the present work to study the structural and electronic properties of stoichiometric In_mP_n ($m = n$) and nonstoichiometric In_mP_n ($m \neq n$) clusters as a function of system size. The experimentally studied systems are very large with $m + n$ ranging from few 10s to several 1000s, which is difficult to tackle in silico.[10] Therefore, in the present work we limited ourselves to a detailed study of a number of different clusters with $n + m$ up to around 200. We considered spherical parts of both wurtzite and zinc blende crystal structures and allowed subsequently each of these clusters to relax to its closest total-energy minimum, whereby all atom were allowed to move. The center of the initial spherical parts was chosen as either the midpoint of an In−P nearest-neighbor bond (leading to stoichiometric clusters) or on an In or P atom (giving nonstoichiometric clusters). By varying *n* and *m*, we can identify some of the trends in the properties of the clusters as functions of their size.

* Corresponding author. E-mail: m.springborg@mx.uni-saarland.de.
[†] E-mail: s.roy@mx.uni-saarland.de.

10.1021/jp0271312 CCC: $25.00
Published on Web 03/04/2003

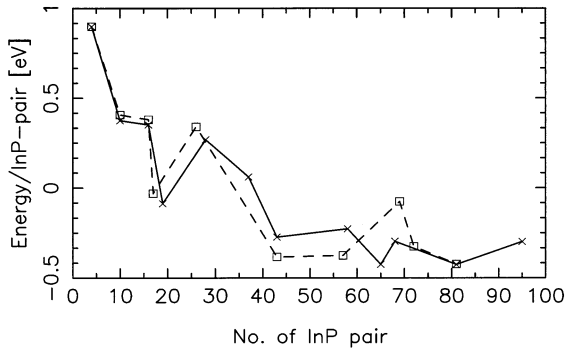

Figure 1. Variation in the total energy per InP pair as a function of number of pairs for stoichiometric zinc blende-derived (solid line) and wurtzite-derived (dashed) clusters.

The paper is organized as follows. Section 2 gives a brief description of the computational method, and our results are discussed in section 3. Finally, our main conclusions are summarized in section 4.

Method of Calculation

We have used a parametrized density-functional tight-binding method that has been described in detail elsewhere.[19−21] According to this method, the binding energy of a given system is written as

$$E_{\mathrm{b}} = \sum_i \epsilon_i - \sum_{jk} \epsilon_{jk} + \frac{1}{2}\sum_{k\neq l} U_{kl}(|\vec{R}_k - \vec{R}_l|) \qquad (1)$$

ϵ_i is the energy of the ith orbital for the system of interest, and ϵ_{jk} is the energy of the j th orbital for the isolated k th atom. Finally, U_{kl} is a pair potential between the k th and l th atom. The valence single-particle eigenfunction $\psi_i(\vec{r})$ to the Kohn−Sham equations $\hat{h}\psi_i = \epsilon_i\psi_i$ are expanded in a set of atom-centered basis functions $\chi_{klm}(\vec{r})$. Here, k denotes the atom and (lm) the angular dependence. The matrix elements $\langle\chi_{k_1l_1m_1}|\hat{h}|\chi_{k_2l_2m_2}\rangle$ and $\langle\chi_{k_1l_1m_1}|\chi_{k_2l_2m_2}\rangle$ are obtained from density-functional calculations on the diatomic molecules. Finally, the pair potentials U_{kl} are determined so that the binding energy curves of the diatomics are reproduced accurately. Only In 5s and 5p as well as in P 3s and 3p electrons were explicitly included in the calculations, whereas all other electrons were treated within a frozen-core approximation. Although it can be argued that also the In 4d electrons should be treated explicitly, for the isolated atom they lie about 5 eV below the P 3s orbitals and, moreover, their effects are indirectly included in the potentials U_{kl}.

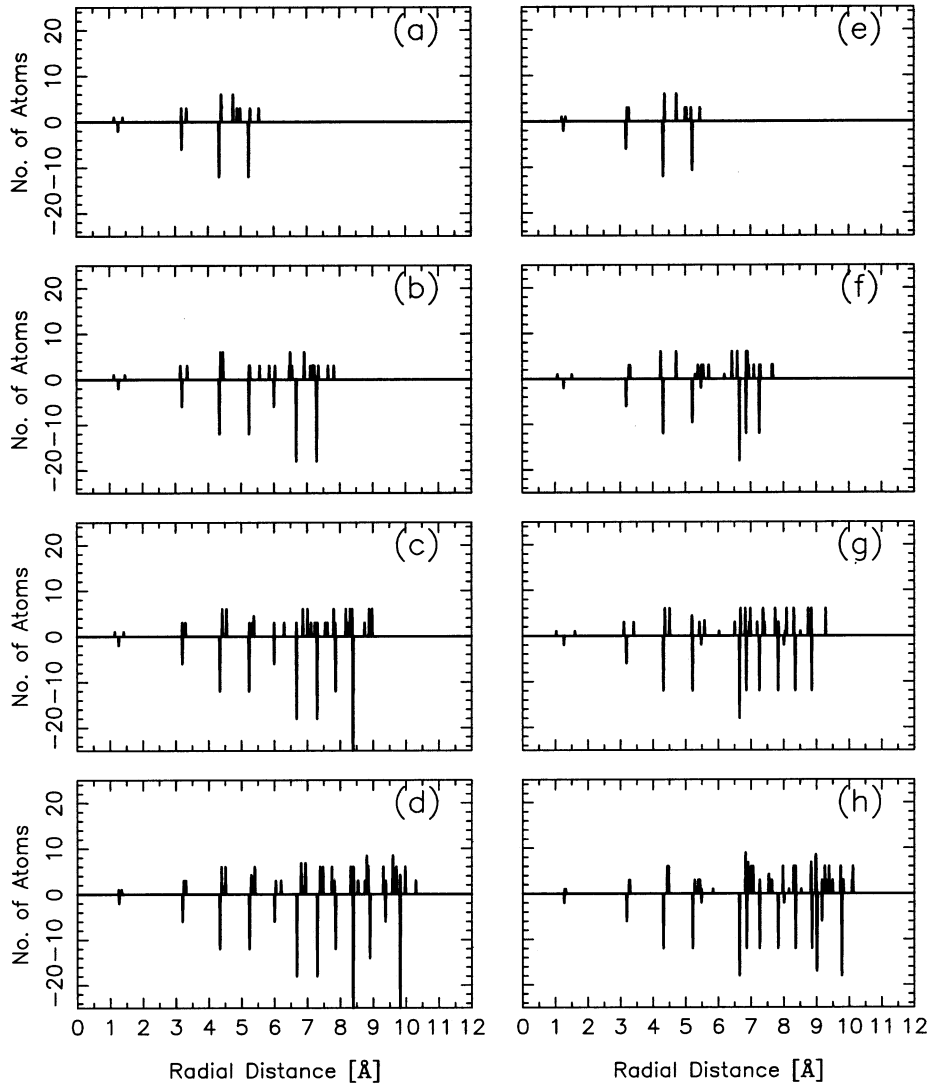

Figure 2. Radial distribution of indium and phosphorus atoms for zinc blende-derived (right column) and wurtzite-derived clusters (left column) of different sizes: (a), (e) $In_{16}P_{16}$; (b), (f) $In_{37}P_{37}$; (c), (g) $In_{57}P_{57}$; (d), (h) $In_{81}P_{81}$. In each panel, the upper part represents the relaxed and the lower part the unrelaxed structure, respectively.

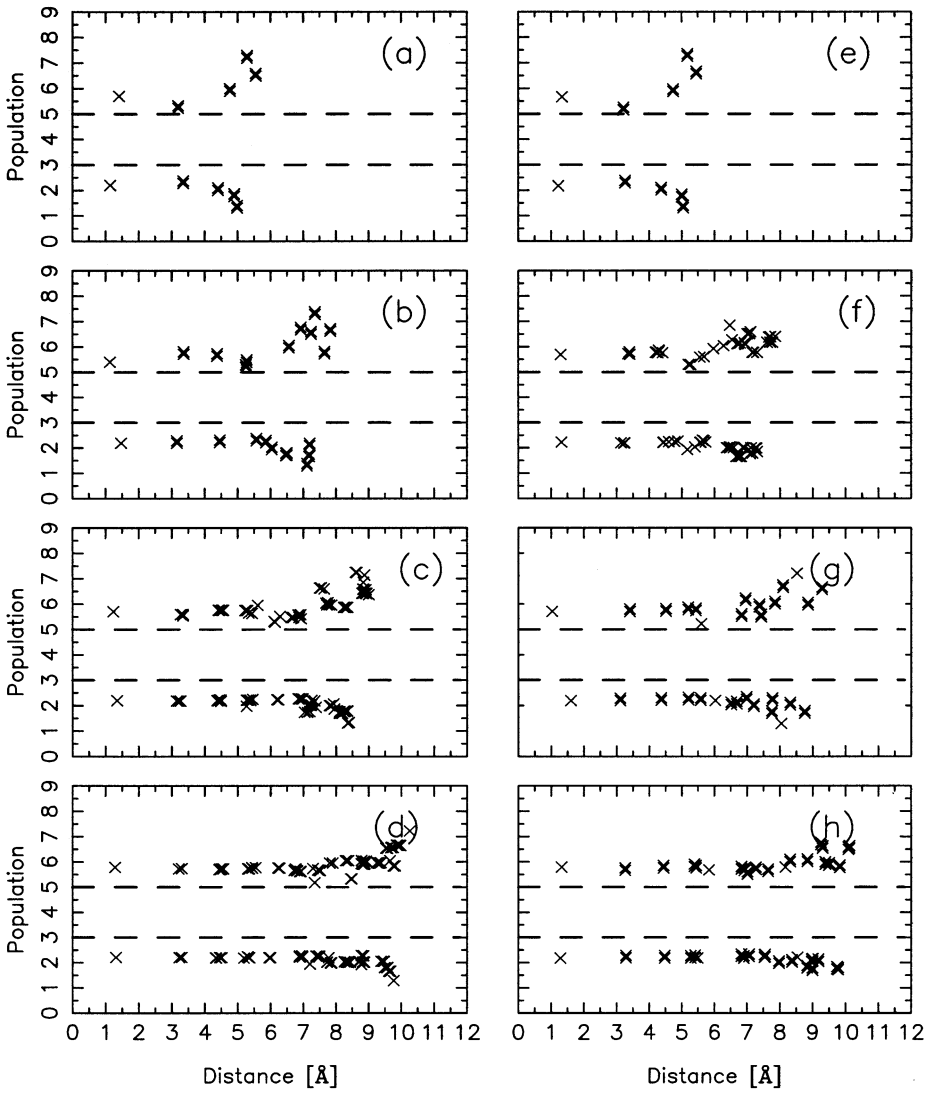

Figure 3. Radial distribution of Mulliken gross populations for the valence electrons of indium and phosphorus atoms for the same structures as in Figure 2. The horizontal dashed lines mark the values for the neutral atoms, i.e., 3 for In and 5 for P.

It is obvious that the approach we are using has been optimized for the smallest possible systems, i.e., in our case the In_2, P_2, and InP diatomic molecules. To test its transferability to larger systems, we studied the infinite zinc blende InP crystal. The lowest total energy was found for a lattice constant of 5.92 Å, whereas the experimental value is 5.87 Å.[22] The good agreement makes us believe that the approach is accurate and that the results for the finite clusters are accurate, too. For the infinite wurtzite InP crystal we found lattice constants of 4.31 and 6.89 Å. This leads to nearest-neighbor bond lengths of 2.55 and 2.58 Å for the two structures, respectively. Finally, the total-energy difference between the two structures was found to be 0.026 eV per InP pair, with the zinc blende structure being the stabler one.

Subsequently, we studied the clusters with up to 200 atoms. For these calculations we started by considering spherical parts of the zinc blende or wurtzite structures with radii up to around 2 nm. The centers were placed either at the midpoint of a In−P bond, giving stoichiometric cluster, or at either an In or a P atom, giving nonstoichiometric clusters. Although experimentally studied systems often possess ligands that passivate dangling bonds on the surfaces, of computational reasons, we chose here to study naked clusters. After the initial structures were defined as described above, each was allowed to relax to its nearest local total-energy minimum. In analyzing the results, we considered both the initial and final structures, whereby the effects of structural relaxations could be identified.

To analyze the results for an In_nP_m cluster, we first determine the center of the cluster,

$$\vec{R}_0 = \frac{1}{n+m}\sum_{j=1}^{n+m}\vec{R}_j \qquad (2)$$

and, subsequently, for each atom its so-called radial distance

$$r_j = |\vec{R}_j - \vec{R}_0| \qquad j = 1, 2, ..., n+m \qquad (3)$$

Finally, we depict various properties (number of atoms, Mulliken gross populations, etc.) as functions of this radial distance for all the atoms of the cluster of interest. In some cases, we will compare the properties for the system before and after structural relaxation. In those cases, we will let upward pointing curves show the results after relaxation and downward pointing curves show the results before relaxation.

Results and Discussion

Stoichiometric Clusters. Figure 1 shows the variation in the total energy per InP pair for stoichiometric In_nP_n clusters as a function of *n*. Although in most cases we do not have clusters

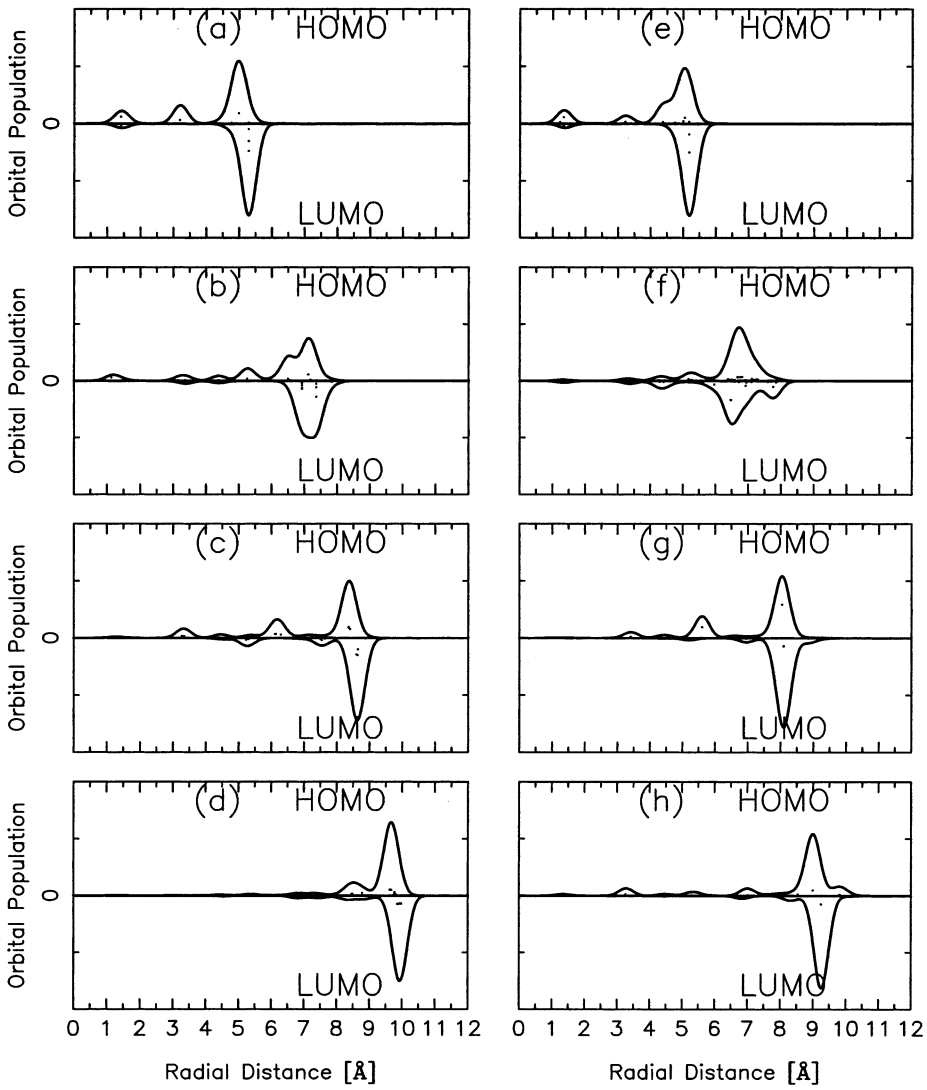

Figure 4. Schematic representation of the radial distribution of the HOMO and the LUMO for the same clusters as in Figure 2. The upper (lower) part of each panel represents the HOMO (LUMO).

derived from the zinc blende and the wurtzite crystal structures of exactly the same size, the results of the figure support the consensus that the relative stability of these two types of clusters is size-dependent. This is in accord with similar results we have obtained earlier for stoichiometric CdS clusters of these two crystal structures[23] and with the fact that our calculated total-energy difference for the infinite crystals for these two structures is small (see above).

Figure 2 shows the radial distribution of the atoms (i.e., the number of atoms with a certain radial distance broadened slightly) for zinc blende-derived (right column) and wurtzite-derived (left column) clusters both before and after structural relaxation. Comparing relaxed and unrelaxed structures clearly shows that in the optimization procedure the maximum changes occur in the surface region. By considering the radial distribution for the In and P atoms individually (not shown), we found that the In atoms move inward whereas the P atoms outward. This tendency for the metal atoms to seek a high coordination and the nonmetal atoms to accept a lower coordination is in agreement with our previous results for naked CdS clusters[23] and with simple chemical intuition.

Finally, in our calculations the structural relaxations were never so large that In−In or P−P nearest-neighbor bonds were found, although this may be a consequence of our chosen initial structures where such bonds are absent, too.

Turning to the electronic properties of the clusters, we show in Figure 3 the Mulliken gross populations for the individual atoms as a function of their radial distance of eq 3. Only the valence electrons are included, i.e., for the neutral atoms these numbers would be 5 for P and 3 for In. It is readily seen from this figure that in the inner part of the clusters there is a small electron transfer from In to P which is largely independent of the radial distance, whereas in the outer region we can define a surface region characterized by an increased electron transfer and having a thickness of about 2.5−3 Å, essentially independent of size of the cluster and of whether it has been derived from the zinc blende or wurtzite crystal structure. Also this finding is in accord with our previous results for CdS clusters.[23] Finally, a careful inspection of Figure 3 reveals that the outermost atoms are P atoms, as mentioned above.

Much of the interest in semiconductor nanoparticles originates from their optical properties. These, in turn, are dominated by excitonic effects, but to a first approximation the excitonic wave functions are first of all determined by the orbitals closest to the gap, i.e., the HOMO and the LUMO. Optical relaxation processes, therefore, depend strongly on the spatial distribution

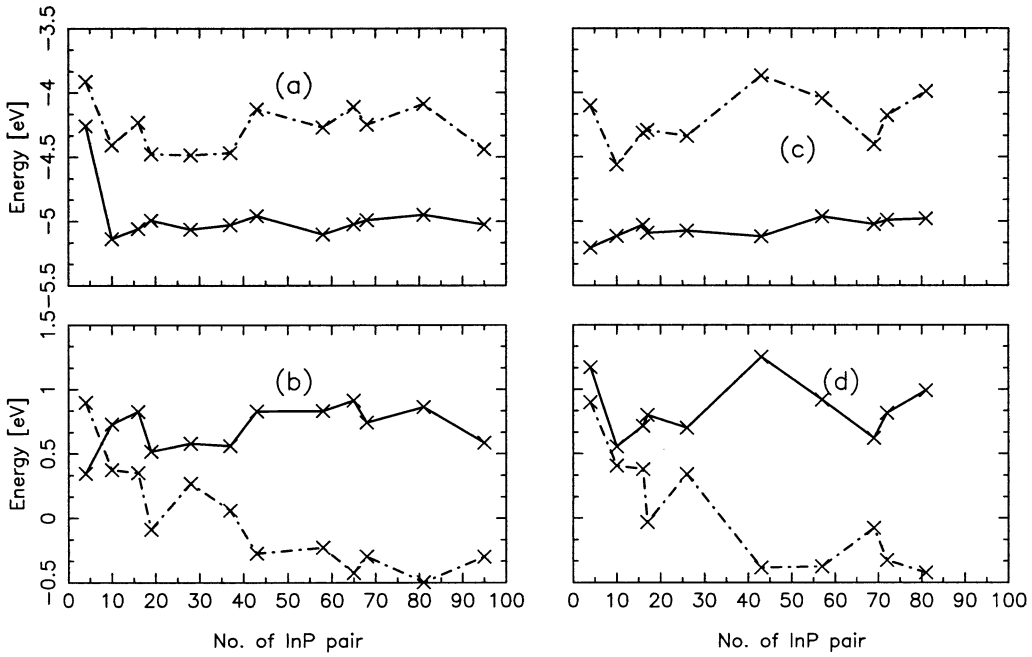

Figure 5. (a), (c) HOMO (lower curve) and LUMO (upper curve) energies as well as (b), (d) HOMO−LUMO gap (solid curve) and relative total energy per InP pair (dashed curve) for stoichiometric zinc blende-derived (left column) and wurtzite-derived clusters (right column) as functions of the number of InP pairs.

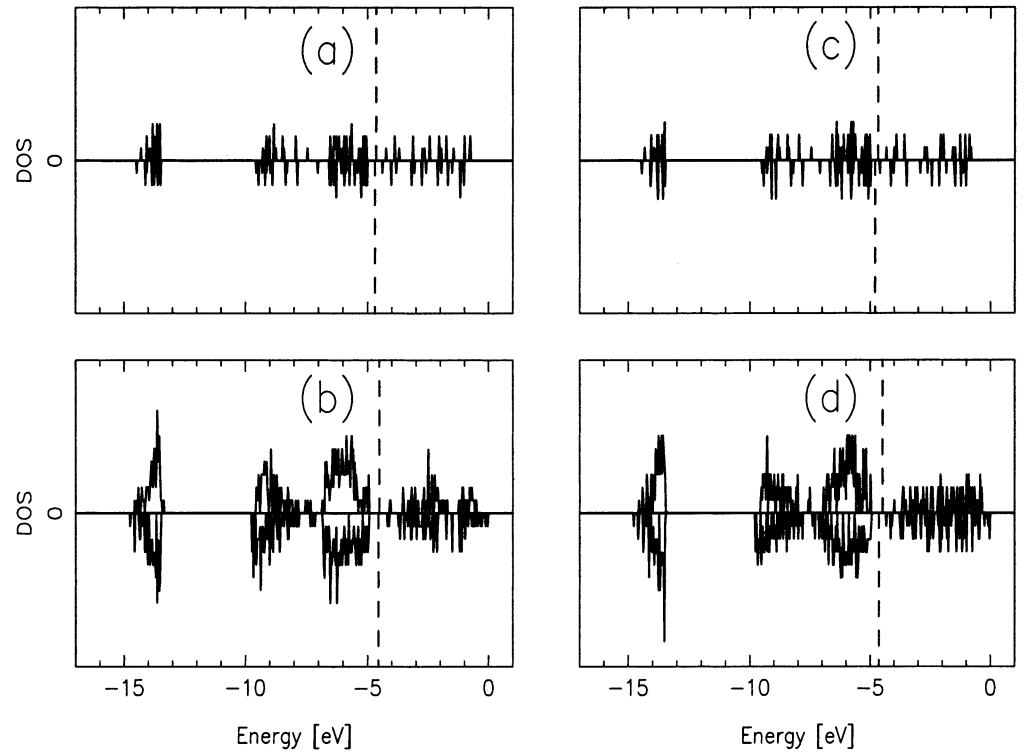

Figure 6. Density of states (DOS) for different zinc blende-derived (right column) and wurtzite-derived (left column) clusters of different sizes: (a), (c) $In_{16}P_{16}$ and (b), (d) $In_{81}P_{81}$. The upper part of each panel represents relaxed and the lower part unrelaxed structures, respectively. The vertical dashed lines mark the Fermi energy.

of these orbitals, and it is highly relevant to analyze these. Here, we will use a qualitative approach as follows.

For any orbital we construct the density

$$\rho_i(\vec{r}) = \sum_j N_{ij}\left(\frac{2\alpha}{\pi}\right)^{3/2} \exp[-\alpha(\vec{r} - \vec{R}_j)^2] \qquad (4)$$

Here, N_{ij} is the Mulliken gross population for the jth atom and ith orbital and α is a fixed constant that is chosen so that it leads to illustrative figures. Finally, we calculate (and depict) the spherical average of this density about the center of the cluster, eq 2. Because we are interested in a qualitative and comparative description of the radial distribution of the orbitals, we choose a fixed value of α for all orbitals and atoms instead of analyzing the true density of each orbital.

Figure 4 shows this representation of the spatial dependences of the HOMO and the LUMO. It is seen that both the HOMO and the LUMO are localized to the outermost regions of the

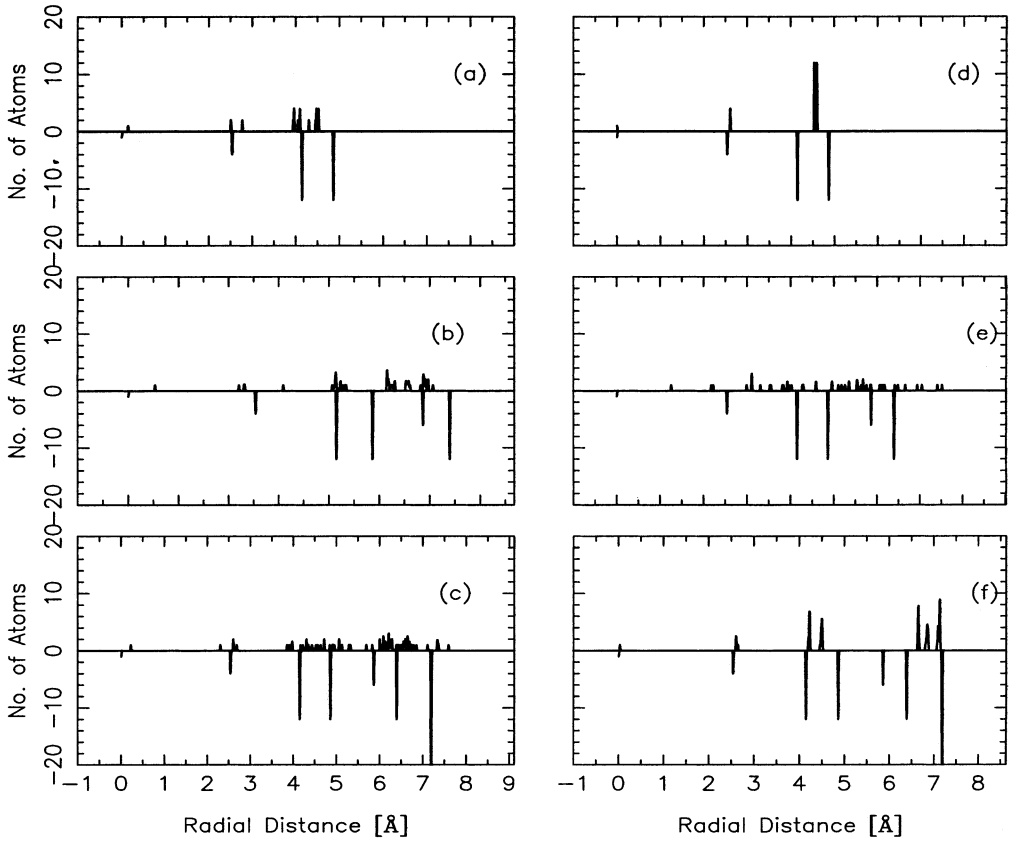

Figure 7. Radial distribution of indium and phosphorus atoms for nonstoichiometric phosphorus-rich (left column) and indium-rich (right column) clusters of different sizes: (a) $In_{13}P_{16}$; (d) $In_{16}P_{13}$; (b) $In_{19}P_{28}$; (e) $In_{28}P_{19}$; (c) $In_{28}P_{43}$; (f) $In_{43}P_{28}$. The upper part of each panel represents relaxed and the lower part unrelaxed structures, respectively.

clusters. In our earlier work on CdS clusters we found a similar localization for the LUMO, but the HOMO was found to be delocalized essentially over the complete cluster.[23] A more careful inspection of Figure 4 shows that the HOMO is localized to regions of slightly smaller values of the radial distance compared with the LUMO, and analyzing the two orbitals in more detail, we found that the HOMO has dominating contributions from the outer In atoms and the LUMO from the outer P atoms. This finding is in contrast to the theoretical results of Fu and Zunger[17] who (using a density-functional, pseudopotential, plane-wave method) examined cubic (unrelaxed) clusters of zinc blende InP for which the surfaces in a first step had been completely passivated. By removing the passivating potentials from the surface In atoms, they found orbitals due to dangling bonds on the outermost In atoms just below the conduction-band edge (i.e., the new LUMO was centered on In), whereas removing these potentials from the outermost P atoms led to extra P-centered orbitals just above the valence-band edge. By analyzing our results, we found that the spatial distribution of the HOMO and LUMO changed only very little upon structural relaxation so that this difference cannot explain the discrepancy between our results and those of Fu and Zunger. On the other hand, as we shall see below, terminating the cluster differently may lead to modifications in these conclusions, so that the discrepancy may be due to the fact that we consider naked clusters, whereas Fu and Zunger have studied clusters where all bonds on the surface were passivated except, at most, for those of a single atom.

Parts a and c of Figure 5 show the variation in the energy of the HOMO and the LUMO as a function of cluster size. Because both orbitals are located to the surface region, they show a clear dependence on the size of the cluster, i.e., on details of the surface. However, as discussed above, there is a small difference between the HOMO and the LUMO with the latter being localized to the absolutely outermost atoms and the former being located to atoms that are slightly more distant from the surface, and, accordingly, the size dependence of the energy of the HOMO is less pronounced as that of the LUMO.

Parts b and d of Figure 5 show the variation in the total energy per InP pair together with the HOMO−LUMO gap. In agreement with results for other systems[23−25] we observe a marked correlation between the energy gap and the total energy: low total energy (large stability) correlates with large HOMO−LUMO gap. This finding may actually be considered related to the HSAB (hard and soft acids and bases) principle:[26] systems are particularly inert (stable) if their hardness is particularly large. As a first approximation, the hardness is simply the HOMO−LUMO energy gap. On the other hand, the correlation between the HOMO−LUMO gap and stability for clusters is more well-known for metal clusters where it is closely related to the occurrence of the so-called magic numbers.[27,28]

It is interesting to see in Figure 5 that the HOMO−LUMO gap converges very fast to a constant value as a function of size, when the size-dependent oscillations are ignored. For other materials, the HOMO−LUMO gap is more like a monotonically decreasing function modulated by the size-dependent oscillations. However, this finding is in perfect agreement with the experimental results of Kolenbrander and Mandich[29] who studied the absorption of very small stoichiometric InP clusters using two-color resonant two-photon dissociation spectroscopy. On the other hand, Banin et al.[30] studied in their experiments passivated clusters and found that the energy gap was a slowly converging function of size. The difference agrees well with our finding that the HOMO and LUMO are located to the

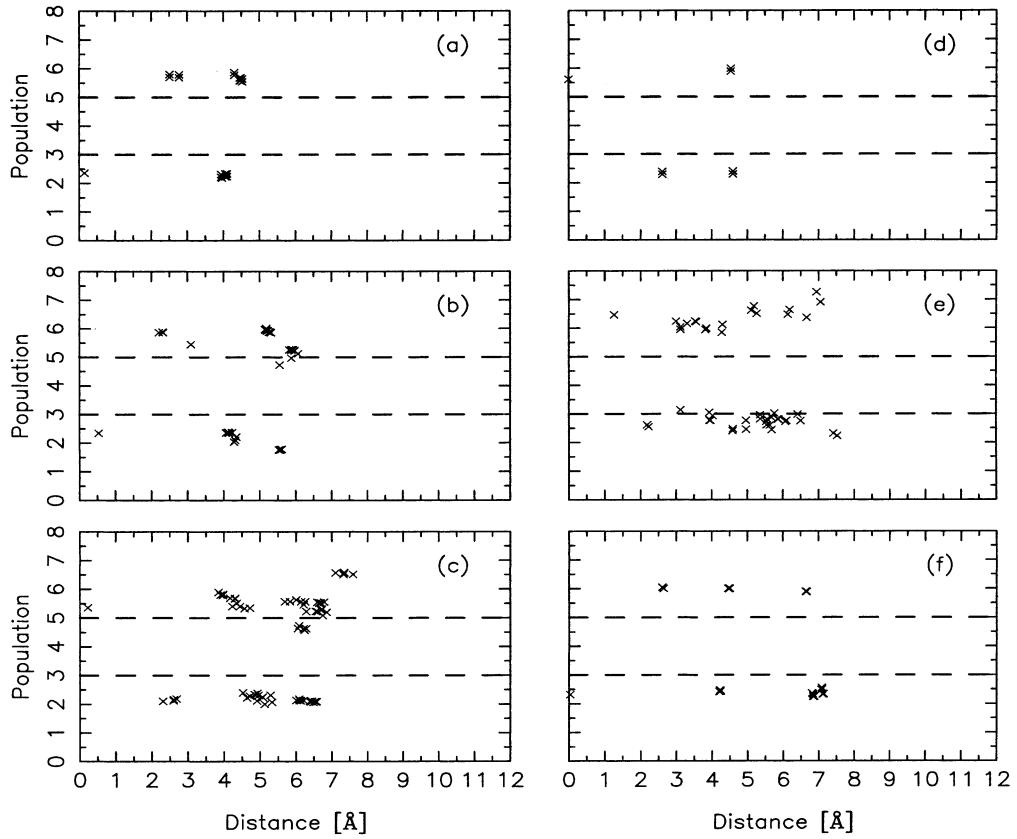

Figure 8. Radial distribution of Mulliken gross populations for the same nonstoichiometric clusters as in Figure 7. The upper part of each panel represents relaxed and the lower part unrelaxed structures, respectively. The dashed lines correspond to the populations of the neutral atoms, i.e., 5 for phosphorus and 3 for indium.

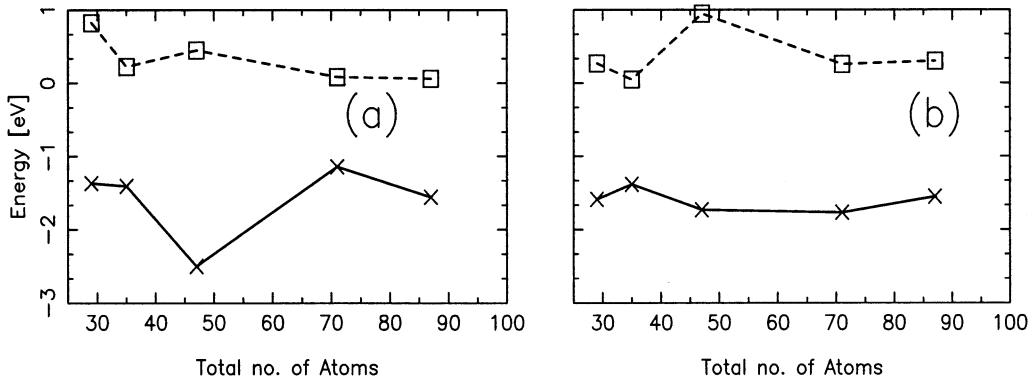

Figure 9. Binding energy per atom (solid curve) and HOMO−LUMO energy gap (dashed curve) for (a) In-rich and (b) P-rich nonstoichiometric clusters as a function of the total number of atoms.

surface atoms and, accordingly, will change energy significantly when the surface is passivated.

Finally, as representative examples, we show in Figure 6 the density of states (broadened by fairly narrow Gaussians) for some few clusters. It is seen that they all have the same overall structure, and, moreover, that the structural relaxation leads to an increase in the HOMO−LUMO gap. Also this latter can be interpreted as a manifestation of the HSAB principle: the hardness and, accordingly, the stability is increased upon increasing the gap. The orbitals in the range between −15 and −13 eV are mainly due to phosphorus 3s functions, those between −10 and −7 eV are due to 4d functions of In, and finally, the band between −6.5 and +5 eV is due to 5s and 5p functions of In and 3p functions of P.

Nonstoichiometric Clusters. In studying the nonstoichiometric clusters, we only considered those derived from the zinc blende crystal structure. We considered a sphere with the center at either an In or a P atom. For the unrelaxed stoichiometric clusters of the preceding subsection, the surfaces contained in all cases the same number of In and P atoms, whereas in the present case the surface is formed exclusively by one type of atoms. Considering a spherical part of a general AB zinc blende crystal with the center at an A atom, the next layer will contain 4 B atoms, then 12 A atoms, followed by 12 B atoms, then 6 A atoms, and 12 B atoms, followed by 24 atoms, and so on. This gives clusters with stoichiometries A, AB_4, $A_{13}B_4$, $A_{13}B_{16}$, $A_{19}B_{16}$, $A_{19}B_{28}$, $A_{43}B_{28}$, ..., which are alternatingly A- and B-rich as well as alternatingly terminated by A and B atoms.

Because these clusters all have different relative number of In and P atoms, it is not possible to compare the stability of the different clusters, as we could do for the stoichiometric clusters (cf. Figure 1).

In Figure 7 we show the radial distribution of the atoms for the systems we have considered. It is clearly seen that for these

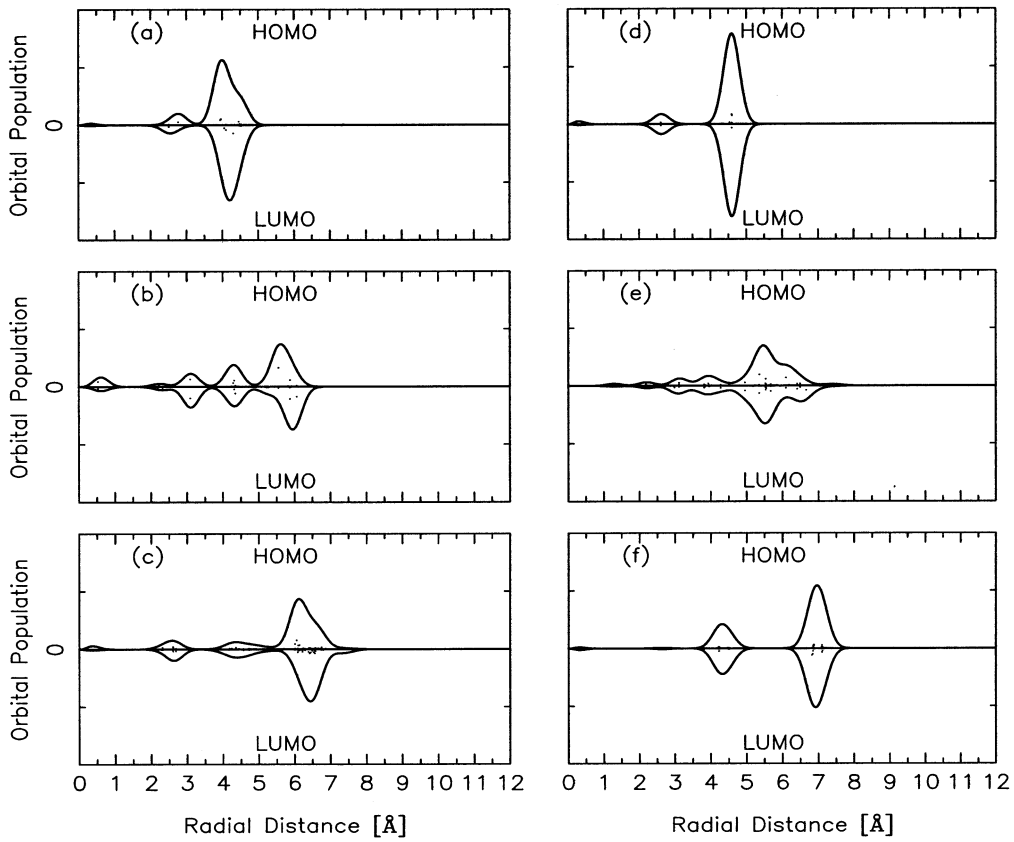

Figure 10. As in Figure 5, but for the nonstoichiometric clusters of Figure 8.

clusters the effects of relaxation are extended throughout the major parts of the clusters. All atoms except for the innermost ones are found to change their positions significantly.

The Mulliken gross populations are shown in Figure 8. Compared to the stoichiometric clusters, the identification of a surface layer characterized by a larger electron transfer between In and P seems not to be directly possible, and instead, there is a scatter of the populations for both types of atoms throughout the entire cluster. In addition, the atoms appear to have a larger average atomic charge for the nonstoichiometric clusters than for the stoichiometric ones.

For the nonstoichiometric clusters, both for P-rich and In-rich ones, the HOMO−LUMO gap is very small. Due to this it is very difficult to identify any correlation between energy gap and stability (cf. Figure 9). The fact that the HOMO−LUMO gap for these nonstoichiometric clusters is smaller than that of the stoichiometric clusters is in agreement with the experimental results of Kolenbrander and Mandich.[29]

Finally, we show in Figure 10 the schematic representation of the radial distribution of the HOMO and LUMO. In this case both frontier orbitals are located on the same atoms and they are both surface states. Thus, both for stoichiometric and nonstoichiometric clusters the frontier orbitals are surface states, independent of whether there is one or two types of atoms on the surface.

Conclusions

In this paper we have reported results of a theoretical study of the electronic and structural properties of stoichiometric and nonstoichiometric naked InP clusters with up to around 200 atoms, i.e., with a diameter of almost 2 nm. The calculations were performed using a simplified LCAO-DFT-LDA-TB scheme. This work represents the first systematic theoretical study of the structural and electronic properties of such a large class of stoichiometric and nonstoichiometric InP (or any other AB semiconductor) clusters.

Our main conclusions are as follows: (a) The structure of a cluster depends critically on the size of the cluster. (b) Both the HOMO−LUMO gap and the total energy per atom is, at least for the smaller clusters of this study, a nonmonotonic function of the size. (c) In the case of stoichiometric clusters there is a clear surface region of about 2.5−3 Å, but we cannot identify any surface region for the nonstoichiometric clusters. (d) There is a correlation between gap and stability for stoichiometric clusters but due to very small gap for nonstoichiometric ones it is difficult to identify this correlation for those. (e) Stoichiometric zinc blende-derived and wurtzite-derived clusters for InP have almost the same energy for finite systems. (f) Finally, both the HOMO and the LUMO are located to atoms near the surface. For the stoichiometric clusters the HOMO has its major components on In atoms and the LUMO its major components on P atoms. (g) For the stoichiometric clusters the total energy per pair is a decreasing function of size modulated by size-dependent oscillations, whereas the HOMO−LUMO gap is essentially a constant modulated by the size-dependent oscillations. Finally, we stress that parts of these results may be modified if we include some solvent or ligands in our calculations instead of considering naked, isolated clusters.

Acknowledgment. This work was supported by the SFB 277 at the University of Saarland. The authors are grateful to Fonds der Chemischen Industrie for a very generous support and to Jan-Ole Joswig for a number of useful discussions.

References and Notes

(1) Steigerwald, M. L.; Alivisatos, A. P.; Gibson, J. M.; Harris, T. D.; Kortan, R.; Muller, A. J.; Thayer, A. M.; Duncan, T. M.; Douglass, D. C.; Brus, L. E. *J. Am. Chem. Soc.* **1988**, *110*, 3046.

(2) Deglmann, P.; Ahlrichs, R.; Tsereteli, K. *J. Chem. Phys.* **2002**, *116*, 1585.
(3) Guden, M.; Piprek, J. *Modelling Simul. Mater. Sci. Eng.* **1996**, *4*, 349.
(4) Kawakami, T.; Okamura, M. *Electron. Lett.* **1979**, *15*, 502.
(5) Ridley, B. K. *J. Appl. Phys.* **1977**, *48*, 754.
(6) Kamimura, K.; Suzuki, T.; Kunioka, A. *Appl. Phys. Lett.* **1981**, *38*, 259.
(7) Hurwitz, C. E.; Hsieh, J. J. *Appl. Phys. Lett.* **1978**, *32*, 487.
(8) Yeh, C.; Lu, Z. W.; Froyen, S.; Zunger, A. *Phys. Rev. B* **1992**, *45*, 12130.
(9) Persall, T. P. *Properties, Processing and Applications of Indium Phosphide*; Inspec: London, 2000.
(10) Billas, I. M. L.; Châtelain, A.; de Heer, W. A. *Science* **1994**, *265*, 1682.
(11) Henglein, A. *Top. Curr. Chem.* **1988**, *143*, 113.
(12) Yoffe, A. D. *Adv. Phys.* **1993**, *42*, 173.
(13) Nirmal, M.; Norris, D. J.; Kuno, M.; Bawendi, M. G.; Efros, A. L.; Rosen, M. *Phys. Rev. Lett.* **1995**, *75*, 3728.
(14) Alivisatos, A. P. *J. Phys. Chem.* **1996**, *100*, 13226.
(15) Weller, H. *Angew. Chem.* **1993**, *105*, 43.
(16) Fu, H.; Zunger, A. *Phys. Rev. B* **1997**, *55*, 1642.
(17) Fu, H.; Zunger, A. *Phys. Rev. B* **1997**, *56*, 1496.
(18) Fu, H.; Zunger, A. *Phys. Rev. B* **1998**, *57*, 15064.
(19) Blaudeck, P.; Frauenheim, Th.; Porezag, D.; Seifert, G.; Fromm, E. *J. Phys. Condens. Matter* **1992**, *4*, 6389.
(20) Porezag, D.; Frauenheim, Th.; Köhler, Th. Seifert, G.; Kaschner, R. *Phys. Rev. B* **1995**, *51*, 12947.
(21) Seifert, G.; Porezag, D.; Frauenheim, Th. *Int. J. Quantum Chem.* **1996**, *58*, 185.
(22) http://www.semiconductors.co.uk/.
(23) Joswig, J.-O.; Springborg, M.; Seifert, G. *J. Phys. Chem. B* **2000**, *104*, 2617.
(24) Springborg, M.; Joswig, J.-O.; Grigoyan, V. G.; Gräf, C.; Roy, S.; Sarkar, P. Ψ_k—*Newsletter* **2002**, *49*, 99.
(25) Joswig, J.-O.; Roy, S.; Sarkar, P.; Springborg, M. *Chem. Phys. Lett.* **2002**, *365*, 75.
(26) Pearson, R. G. *Chemical Hardness*; Wiley-VCH: Weinheim, Germany, 1997.
(27) Knight, W. D.; Clemenger, K.; de Heer, W. A.; Saunders, W. A.; Chou, M. Y.; Cohen, M. L. *Phys. Rev. Lett.* **1984**, *52*, 2141.
(28) Ekardt, W. *Phys. Rev. B* **1984**, *29*, 1558.
(29) Kolenbrander, K. D.; Mandich, M. L. *Phys. Rev. Lett.* **1990**, *65*, 2169.
(30) Banin, U.; Cerullo, G.; Guzelian, A. A.; Bardeen, C. J.; Alivisatos, A. P.; Shank, C. V. *Phys. Rev. B* **1997**, *55*, 7059.